ACS OMEGA

Open Access

http://pubs.acs.org/journal/acsodf

Article

Comparison of the Effect of Kaolin and Bentonite Clay (Raw, Acid-Treated, and Metal-Impregnated) on the Pyrolysis of Waste Tire

Mahmudur Rahman,* Muhammad Omar Faruk, Md Waliul Islam, Moni Akter, Joyanta K. Saha, Nafees Ahmed, Ayesha Sharmin, Md. Azizul Hoque, Mirola Afroze, Mala Khan, Umme Sarmeen Akhtar, and Md Mainul Hossain

Cite This: *ACS Omega* 2024, 9, 474−485

Read Online

ACCESS | Metrics & More | Article Recommendations | Supporting Information

ABSTRACT: This study investigates the effectiveness of kaolin and bentonite catalysts in improving liquid hydrocarbon yields during the pyrolysis of waste tires. Raw clay, nitric acid-treated clay, and mono- or bimetal-impregnated clay were used as catalysts in the pyrolysis of waste tire. Acid-treated kaolin produced a higher yield of liquid hydrocarbons (43.24−47%) compared to acid-treated bentonite (35.34−41.85%). This improvement in the liquid yield can be attributed to the higher specific surface area and pore diameter of the acid-treated clay in comparison to raw kaolin (39.48%) and raw bentonite (31.62%). Moreover, the use of metal-impregnated catalysts, such as Fe/kaolin and Ni/Fe/kaolin, resulted in higher liquid yields (47%) compared to the 3 M HNO_3-treated kaolin catalyst (43.24%). Gas chromatography−mass spectrometry (GC-MS) analysis confirmed the presence of limonene, a crucial ingredient for commercial perfume production, in the liquid products. The calorific values of oil obtained through kaolin and bentonite catalysis were measured at 13,922 and 10,174 kcal/kg, respectively, further highlighting the potential of these catalysts in waste tire valorization.

INTRODUCTION

The disposal of waste tires poses a significant environmental challenge, characterized by their nonbiodegradability and the need for extensive land sites to accommodate their large volume.[1] The annual production of waste tires all over the world is about 1.5 billion.[2] Bangladesh, as a developing country, faces a good share of the waste tire disposal problem, producing a staggering 90,000 t of scrap tires each year.[3] It is predicted that the amount of waste tires in Bangladesh might increase to 150,000 t within the next couple of years. Improper tire disposal practices, such as open dumping and landfills, not only occupy valuable land resources but also create ideal breeding grounds for disease-carrying mosquitoes, leading to deadly diseases like malaria and dengue. In an effort to address this mounting tire waste problem, a small fraction of the scrap tire in Bangladesh undergoes thermal pyrolysis, yielding valuable products such as liquid oil and pyrolytic char. The resulting pyrolytic oil is used as fuel in boilers, while the pyrolytic char serves as a solid fuel source in brickfields. Additionally, pyrolytic char can be further utilized for the production of activated carbon and printer ink. In terms of compositions, tires are made of natural rubber (NR) and synthetic rubber such as styrene−butadiene rubber (SBR) and butadiene rubber (BR) and other ingredients such as vulcanization accelerators, carbon black fillers, strengtheners, metal reinforcements, zinc oxide, sulfur, plasticizers, and antiaging substance. In the tire manufacturing process, vulcanization reactions occur, involving the bonding of rubber polymers with sulfur, imparting the desired strength and elasticity to the tires. On average, the sulfur content in tires amounts to approximately 1.5 wt %. Car and truck tires exhibit variations in their composition, with car tires comprising 14−30% NR, 14−27% synthetic rubber, 20−28% carbon black, 13−25% steel, and 10−17% other materials, such as fabric, fillers, accelerators, and antiaging substances.[4] Truck tires, in contrast, have a higher proportion of NR, accounting for 27 wt %, while synthetic rubber constitutes 14 wt %. Passenger car tires, on the other hand, consist of 14% NR and 27% synthetic rubber.[5]

Different types of valuable products such as pyrolysis oil (TPO), carbon black, and steel wire could be generated by the pyrolysis of waste tires. The optimum temperature of tire pyrolysis is 500 °C.[5] The pyrolysis of tires comprises primary polymer degradation and several secondary reactions. In primary degradation, the main chain scission and depolyme-

Received: August 12, 2023
Revised: December 2, 2023
Accepted: December 7, 2023
Published: December 27, 2023

rization occur. Subsequently, various secondary reactions transform the products of primary degradation into diverse substances. During pyrolysis, additives and plasticizers decompose at above 200 °C while NR decomposes at 200−300 °C and synthetic rubber at 250−500 °C. At temperatures ranging from 500 to 900 °C, the Diels−Alder reaction occurs, leading to the production of limonene, a dimer of isoprene.[2] The liquid fraction obtained by thermal pyrolysis of tires contains various aromatic compounds such as benzene, toluene, xylenes (BTX), and limonene. With a heating value of 44 MJ/kg, pyrolysis oil exhibits potential as an attractive fuel choice.[2] Moreover, the pyrolysis process generates hydrogen and C1−C4 hydrocarbons with higher calorific values, predominantly comprising H_2, H_2S, CO, CO_2, CH_4, C_2H_4 (ethylene), C_3H_6 (propylene), and other hydrocarbons. This gas mixture has the potential to generate power to perform the pyrolysis process as well as for the generation of heat and electricity.

In recent years, state-of-the-art technologies have been applied on tire pyrolysis. For example, different reactors such as fluidized beds, spouted beds, fixed beds, and auger reactors have been explored in tire pyrolysis. Yu et al.[6] conducted the pyrolysis-catalytic upgrading experiments in a two-stage fixed bed reactor where vulcanized rubber was pyrolyzed at the temperature up to 470 °C. A semibatch reactor made from stainless steel 316 with a diameter of 5 cm and length of 19 cm was used for the pyrolysis of tire waste.[7] Duanguppama et al.[8] used a fluidized bed reactor with an internal width and heights of 100 and 800 mm, respectively, made up of stainless steel was introduced to perform the catalytic pyrolysis of *Leucaena leucocephala*. These authors also used a fixed bed reactor as a secondary reactor for upgrading the pyrolysis vapor. The TRL-5 single-auger reactor of 3 m long and divided into three heating zones was used during pyrolysis of end-of-life tires.[9] A tapered spout bed reactor was used to study the continuous pyrolysis of waste truck tires in the range of 425−575 °C by Lopez and his co-workers.[10] This kind of reactor was found to obtain up to 58 wt % yields of pyrolysis oil.

Kaminsky[11] investigated thermal pyrolysis of 1500 kg of tires (over 150 whole tires) in a rotary kiln reactor. The compositions of the pyrolysis products were 18−25 wt % of gas, 25−30 wt % of oil, 35−45 wt % of carbon black and filler materials, and 8−12% of steel cord. Banar et al.[12] carried out pyrolysis of tires at 400 °C. They reported their pyrolysis product compositions to be 38.8 wt % oil, 27.2 wt % gas, and 34 wt % char. Unapumnuk et al.[13] investigated the pyrolysis of tire in a thermal process between 400 and 1000 °C under a nitrogen atmosphere identifying alkylated isomers of cyclohexene, benzene, naphthalene, indan, and styrene in the pyrolysis oil. The major compounds that are present in their pyrolysis oil were benzene, 1,4-dimethyl; benzene, 1-ethyl-2-methyl; benzene, 1-isopropyl-2-methyl; cyclohexene-4-isopropenyl-1-methyl; styrene, R-2-dimethyl; benzene, 1-methyl-4-(1-methylpropyl); indan, 4,7-dimethyl; indene, trimethyl; and naphthalene, 1,3-dimethyl.

Researchers have investigated several catalysts to improve the quality of the pyrolysis oil by increasing the number of desirable compounds such as single-ring aromatic compounds (e.g., benzene, toluene, and *o*-, *m*-, and *p*-xylenes) and light olefins while concurrently reducing sulfur-containing compounds.[4] Among the studied catalysts for tire pyrolysis are catalysts such as ZSM-5 zeolite,[14] Y-zeolite,[14] MCM-41,[15] Ru/MCM-41,[15] spent FCC catalyst,[1] and NaOH.[16]

In comparison to the ZSM-5 catalyst, the Y-zeolite catalyst can produce higher amounts of benzene, toluene, xylenes, naphthalene, and alkylated naphthalenes.[14] However, the addition of a zeolite catalyst led to a reduction in oil generation. For example, without a catalyst, the oil yield was 55.8 wt %, with 38.1 wt % char and 6.1 wt % gas. On the other hand, the addition of the Y-zeolite catalyst resulted in a lower oil yield of 32.2 wt % compared to 38.7% for without the catalyst while the gas yield increased from 16.3 to 21.8 wt %.[14] With the addition of the ZSM-5 catalyst, the oil yield decreased from 42.9 wt % (430 °C) to 34.6 wt % (600 °C) with increasing temperature.[14] Dũng et al.[15] investigated MCM-41 and Ru-MCM-41 catalysts on tire pyrolysis. They also reported a lower oil yield and a higher gas yield in the presence of catalysts. However, the Ru-MCM-41 catalyst exhibited a four-times higher concentration of light olefins and a higher concentration of single-ring aromatic compounds compared to the noncatalytic process. Unfortunately, these catalysts were deactivated due to coke deposition. Therefore, it is essential to develop a coke-resistant and cost-effective catalyst to enhance the economic viability of catalytic pyrolysis.

Clays such as kaolin and bentonite are natural aluminosilicates and are less acidic. Kaolin and bentonite contain a significant amount of SiO_2 and Al_2O_3 and can be used as catalysts in tire pyrolysis. Notably, kaolin[17] and bentonite[18] have been recognized as effective catalysts in the pyrolysis of polyethylene. Luo et al.[19] used clay catalysts such as kaolin (with different particle size) and montmorillonite (MTT) (modified with $ZnCl_2$ and HCl) on the pyrolysis of waste tire. They found that clay catalysts improved the quality and yield of the liquid oil. They also found that $ZnCl_2$-modified MTT promoted aromatization and deoxidation. Their clay catalysts promoted the alkylation of aromatic hydrocarbons and formation of C_{12} to the C_{20} hydrocarbon. In this study, we conducted a comparative study of nitric acid-treated kaolin and bentonite catalysts on tire pyrolysis to understand their effect on oil yield, the compositions of the oil, and the formation of a valuable product like limonene. In addition to the acid treatment of kaolin and bentonite, monometals (Fe and Ni) and bimetals (Fe/Ni) have been impregnated separately into kaolin and bentonite for using as catalysts during the pyrolysis of the waste tire and aiming to understand the influence of the presence of metals on oil yield and compositions.

MATERIALS

Waste tires were collected from Dhaka city, Bangladesh. According to elemental analysis, the waste tire consists of 85.26% C, 7.84% H, 0.50% N, 1.40% S, and 1.19% O and 3.81% inorganic fillers. Kaolin clay was purchased from Rajasthan, India. Bentonite was purchased from Loba Chemie, India, and nitric acid was purchased from Sigma-Aldrich, Germany.

Preparation of Catalysts. *Acidic Treatment of Kaolin and Bentonite.* Acid treatment of both kaolin and bentonite catalysts was conducted by following a similar method. A total of 40 g of the catalyst (kaolin or bentonite) was mixed to 400 mL of 3 M HNO_3 in a 1000 mL round-bottom flask, refluxed for 4−5 h at 120−130 °C, and then cooled and filtered. The filtered solid was then washed and dried at 100 °C for 12 h. Subsequently, the dried solids were calcined at 550 °C for 14 h. The mass of the calcined product dried solid was 23 and 24 g for 3 M HNO_3 treated kaolin and 3 M HNO_3 treated bentonite, respectively. The preparation of 5 M HNO_3-treated

https://doi.org/10.1021/acsomega.3c05951
ACS Omega 2024, 9, 474−485

kaolin and 5 M HNO_3-treated bentonite followed a similar procedure, with the only difference being the use of 5 M HNO_3 instead of 3 M HNO_3. The mass of the catalyst obtained for the treatment with 5 M HNO_3 was 19 g for kaolin and 21 g for bentonite catalysts.

Preparation of Monometallic Catalysts. In this study, monometal was impregnated with 3 M nitric acid-treated bentonite, following the incipient wetness method.[20,21] At first, bentonite was treated with 3 M HNO_3 and then mixed with $FeCl_3{\cdot}3H_2O$ at a mass ratio of approximately 0.05 (e.g., 100.0 g of bentonite contained 5.0 g of Fe metal). 15.0 g of nitric acid-treated bentonite was dissolved in 200 mL of deionized water. The solution was heated at 120 °C for 30 min. Separately, a solution of ferric (III) chloride was prepared by dissolving 2.17 g of $FeCl_3{\cdot}3H_2O$ in 100 mL of water. Followed by the heating step, ferric (III) chloride was added and mixed thoroughly with a continuous stirrer to evaporate the water. When most of the water evaporated from the solution, the remaining mixture was heated at 100 °C (12 h) and calcined at 550 °C (4 h). After the calcination steps, the iron-impregnated bentonite was obtained. Similarly, Fe/kaolin, Ni/bentonite, and Ni/kaolin catalysts were prepared by using the same method with metal precursors such as $FeCl_3{\cdot}3H_2O$ and $Ni(NO_3)_2.6H_2O$.

Preparation of Bimetallic Catalysts. The Ni/Fe/bentonite catalyst was prepared in two steps according to the method reported by Al-Asadi et al.[22] First, the Fe/bentonite suspension was prepared and then a hydrated nickel nitrate solution was added for impregnation. The Fe/bentonite suspension was prepared by adding 7.0 g of Fe/bentonite in 150 mL of distilled water, heating, and stirring continuously for 30 min at 130 °C. After 30 min, the hydrated nickel nitrate solution was added. The hydrated nickel nitrate solution was prepared by dissolving 1.214 g of Ni $(NO_3)_2{\cdot}6H_2O$ in 100 mL of distilled water. After the hydrated nickel solution was added to the Fe/bentonite suspension, the mixture was continuously heated and stirred for another 4 h at 130 °C. The water from the solution was allowed to evaporate at 100 °C (14 h), the produced solid mixture was allowed to be calcined at 550 °C (4 h), and the bimetallic catalyst was produced. In the final bimetallic catalyst, the mass ratio of m(Ni)/m(Fe/bentonite) was approximately 0.035 (i.e., 3.5 g of Ni metal to 100 g Ni/bentonite). Following similar preparation steps, the Ni/Fe/kaolin catalyst was produced, using Fe/kaolin and $Ni(NO_3)_2{\cdot}6H_2O$.

Characterization of Catalysts. Different characterization techniques, such as X-ray powder diffraction (XRD), scanning electron microscopy (SEM), and X-ray fluorescence (XRF), were used to analyze the catalysts prepared. For XRF analysis, 1 g of catalyst was mixed with boric acid (0.25 g). The mixture was pelletized and then analyzed with Lab Center XRF-1800 (Shimadzu, Japan) with an irradiation source of an Rh X-ray at 140 mA and 30 kV. For XRD analysis, a GNR Explorer XRD with a source of Cu−Kα_1 at 35 kV and 25 mA and a step size of 0.1° with data integration time 3 s per step over an angular range of 5−80° (2θ) was used. The XRD and XRF analyses of kaolin and bentonite (in the raw state, after treatment with 3 and 5 M nitric acid treatment and Fe and Ni metal impregnation) were conducted. The BET-specific surface area and pore volume were determined by measuring nitrogen adsorption−desorption isotherms at liquid N_2 temperature (−196 °C) with a PMI BET Sorptometer (BET-201A, USA) apparatus. Evaluation of the BET surface area and pore size distribution were completed with BETwin software. The catalysts for conducting BET analysis were degassed at 120 °C under a vacuum for 1.5 h. Nitrogen adsorption−desorption was carried out for raw kaolin, raw bentonite, 3 and 5 M HNO_3-treated kaolin, and 3 M HNO_3-treated bentonite. For SEM images, the JEOL-SEM 7600F (with an energy-dispersive X-ray spectrometry detector at 5 kV) was used. SEM of raw kaolin, raw bentonite, and 3 and 5 M HNO_3-treated kaolin and bentonite, respectively, were obtained for comparison.

Characterization of Liquid Products. The liquid products were analyzed by GC-MS, FTIR, and ^{1}H NMR spectroscopy. For FTIR analysis, the Shimadzu 8400S (Japan) with KBr (heated at 100 °C for 1 day before analysis) pellets in the range 400−4000 cm^{-1} was used. The Shimadzu GCMS-TQ8040 with a quadrupole mass analyzer for GC-MS/MS analysis and the electron impact ionization technique for MS detection (full scan mode 50−550 m/z) were used. A liquid sample of 0.5 μL was injected in splitless mode (flow rate of 1 mL/min and run time of 30 min) by a capillary column Rxi-5 ms of 30 m length × 0.25 mm id at 250 °C. The oven temperature was set to 50 °C for 1 min and increased to 150 °C at a rate of 5 °C/min and then to 300 °C at 15 °C/min. Different compounds were identified, using the computer-assisted mass spectral search by NIST-MS Library 2009. The ^{1}H NMR of liquid products was conducted by the Bruker model (Avance III HD, 400 MHz). The flash point was determined by a Seta PM-93 instrument. The Seta PM-93 is capable of determining flash points in an automatic manner. The heating value of the produced fuel was determined by a CAL2K-ECO bomb calorimeter. The density, kinematic viscosity, and pour point of the liquid were determined by the Tamson ASTM D1298, ASTM D445, and ASTM D97 methods, respectively.

Tyre Pyrolysis Using Raw, Acid-Treated, and Metal-Impregnated Kaolin and Bentonite Catalysts. 50 g of the waste tire was pyrolyzed in a stainless-steel reactor. The reactor has a length, internal diameter, and outer diameter of 100, 75, and 77 mm, respectively[18] (Figure 1). The reactor consists of

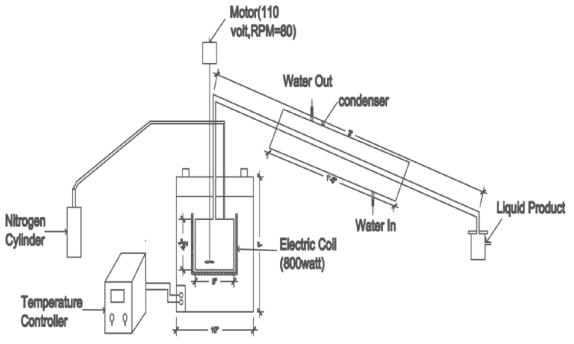

Figure 1. Reactor setup for tire pyrolysis.

an electric furnace for heating, a thermocouple to determine the sample temperature, a temperature controller to maintain a constant temperature, a condenser for excess heat removal and condensation, and a liquid collection vessel for sampling. The reactor is heated by an electric coil of 220 V (1200 W) at a heating rate of 16 °C/min under a nitrogen atmosphere. The stirrer rotation is 30 rpm.

Before conducting pyrolysis experiments, the reactor was rinsed with acetone and then purged with nitrogen gas. The catalysts and waste tires were fed at a mass ratio of 1:10 to the reactor. The reactor was purged with N_2 gas one more time to

https://doi.org/10.1021/acsomega.3c05951
ACS Omega 2024, 9, 474−485

Table 1. Compositions (%) of Raw, Acid-Treated, and Metal-Impregnated Kaolin by XRF

kaolin	SiO_2	Al_2O_3	K_2O	Fe_2O_3	MgO	TiO_2	Na_2O	NiO	Si/Al
raw kaolin (%)	62.56	30.72	4.35	1.23	0.46	0.11	0.09		3.58
3 M HNO_3 treated	64.33	30.08	3.90	0.91	0.52	0.09			3.77
5 M HNO_3 treated	65.53	28.99	3.84	0.87	0.46	0.12	0.11		3.98
Ni/kaolin	64.83	31.43	1.72	0.52				4.20	3.63
Fe/kaolin	65.12	30.67	1.65	4.73	0.49		0.1		3.74
Ni/Fe/kaolin	63.87	29.78	2.39	6.68				4.47	3.77

Table 2. Composition (%) of Raw, Acid-Treated, and Metal-Impregnated Bentonite by XRF

bentonite	SiO_2	Al_2O_3	K_2O	Fe_2O_3	MgO	TiO_2	Na_2O	CaO	NiO	Si/Al
raw bentonite (%)	53.64	13.61	1.60	3.33	2.54	3.19	4.26	1.18		6.94
3 M HNO_3 treated	69.48	10.82	1.37	2.45	1.58	3.43	1.80	0.52		11.34
5 M HNO_3 treated	85.06	6.10	1.40	2.33	0.40	4.11	0.31	0.09		24.64
Ni/bentonite	68.12	11	0.96	2.67	1.75	2.42	0.47		5.19	10.90
Fe/bentonite	67.40	10.20	0.73	4.90	1.20	1.95				11.67
Ni/Fe/bentonite	68.40	10.30	0.61	6.20	0.98	1.84			4.24	11.71

remove any atmospheric oxygen that might have been present in the reaction chamber. Throughout the experiments, supply on N_2 was continued to sustain an oxygen-free atmosphere. Pyrolysis experiments were conducted at a 500 °C temperature and continued for an hour. To remove sulfur, $Ca(OH)_2$ was added to 3 M HNO_3 acid-treated kaolin and bentonite (5 g of catalyst and 5 g of $Ca(OH)_2$ were added in each experiment). The yield (wt %) of liquid was calculated based on eq 1.

$$\text{yield(wt \%)} = \frac{\text{mass of product}}{\text{mass of starting material}} \times 100\% \quad (1)$$

Since the scope of this study was limited to analyzing the liquid fractions of the pyrolysis products, gaseous molecules were vented off without further analysis. As a result of the catalytic decomposition of tires, some coke deposition was observed on the surface of the catalysts. Due to this coke deposition, each catalyst was used only once.

RESULTS AND DISCUSSION

Characterization of the Catalysts. The compositions of raw kaolin and raw bentonite and their corresponding nitric acid-treated and metal-impregnated clays were determined by XRF (Tables 1 and 2). The raw kaolin comprises 62.56% SiO_2 and 30.72% Al_2O_3. On the other hand, raw bentonite contains 53.64% SiO_2 and 13.61 Al_2O_3. The Si/Al ratios of raw kaolin and raw bentonite are 3.58 and 6.94, respectively. The raw kaolin and raw bentonite were treated with 3 and 5 M HNO_3 to modify the Si/Al ratio. Nitric acid reacts with kaolin and bentonite according to eq 2.

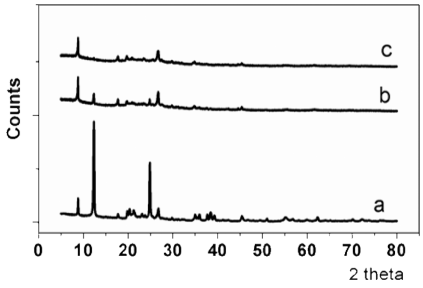

Figure 2. XRD of kaolin clay: (a) raw kaolin, (b) 3 M HNO_3-treated kaolin, and (c) 5 M HNO_3-treated kaolin.

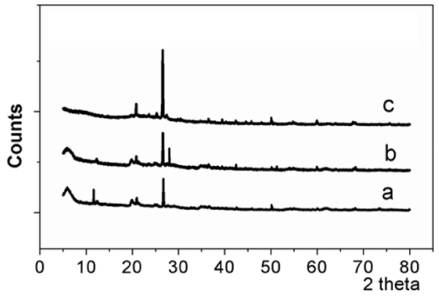

Figure 3. XRD of bentonite: (a) raw bentonite, (b) 3 M HNO_3-treated bentonite, and (c) 5 M HNO_3-treated bentonite.

$$Al_2O_3{\cdot}2SiO_2{\cdot}2H_2O + 3HNO_3 \rightarrow Al(NO_3)_3 + +2SiO_2 + 5H_2O \quad (2)$$

A gradual decrease of Al_2O_3 has been observed with the increase in nitric acid concentration (Tables 1 and 2). For example, after treatment with 3 and 5 M HNO_3, the Al_2O_3 content in kaolin reduced to 30.08 and 28.99%, respectively, resulting in Si/Al ratios of 3.77 and 3.98 compared to raw kaolin. Similarly, in bentonite, the Al_2O_3 content decreased to 10.82 and 6.10% after treatment with 3 and 5 M HNO_3, leading to Si/Al ratios of 11.34 and 24.64 compared to raw bentonite. In the Ni/kaolin and Fe/kaolin catalysts, the percentages of NiO and Fe_2O_3 are 4.20 and 4.73% respectively. In the Ni/bentonite and Fe/bentonite catalysts, the percentages of NiO and Fe_2O_3 are 5.19 and 4.90%, respectively.

Figures 2 and 3 show the XRD patterns of raw kaolin, raw bentonite, and their corresponding HNO_3-treated clays. Raw kaolin is a crystalline material containing 88.5% kaolinite and 11.5% illite, with characteristic peaks at 2θ values of 12.37 and 25° for kaolinite and 8.87 and 17.79° for illite. Acid treatment reduced the peak intensity of the clay, attributed to structural disorder caused by HNO_3 treatment.

The raw bentonite comprises 87.5% quartz and 12.5% montmorillonite. The characteristic peak of bentonite was observed at 2θ values of 5.91, 12.37, 19.85, and 20.87°. The intensity of the diffraction peaks of MTT decreased with an increasing concentration of nitric acid. The XRD patterns of monometals (Ni and Fe) and bimetals (Ni/Fe) impregnated

https://doi.org/10.1021/acsomega.3c05951
ACS Omega 2024, 9, 474−485

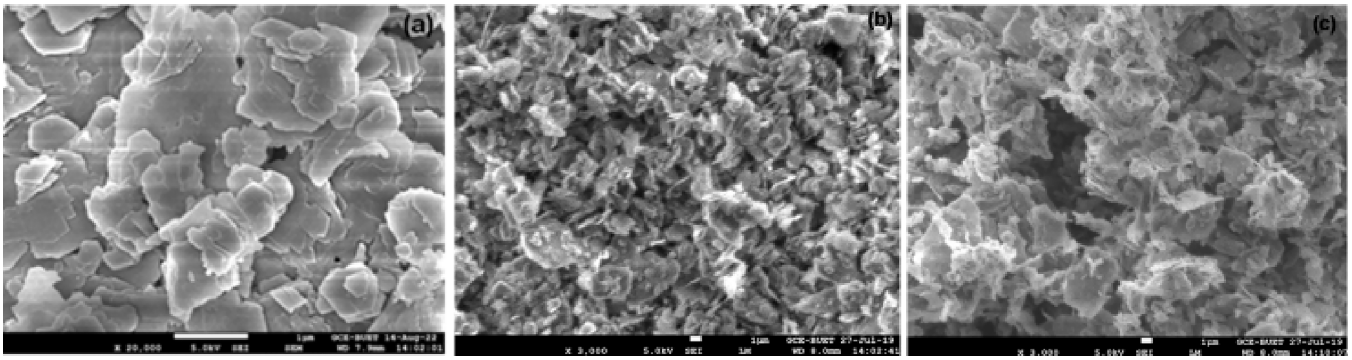

Figure 4. SEM images of (a) raw kaolin clay, (b) 3 M HNO_3-treated kaolin, and (c) 5 M HNO_3-treated kaolin.

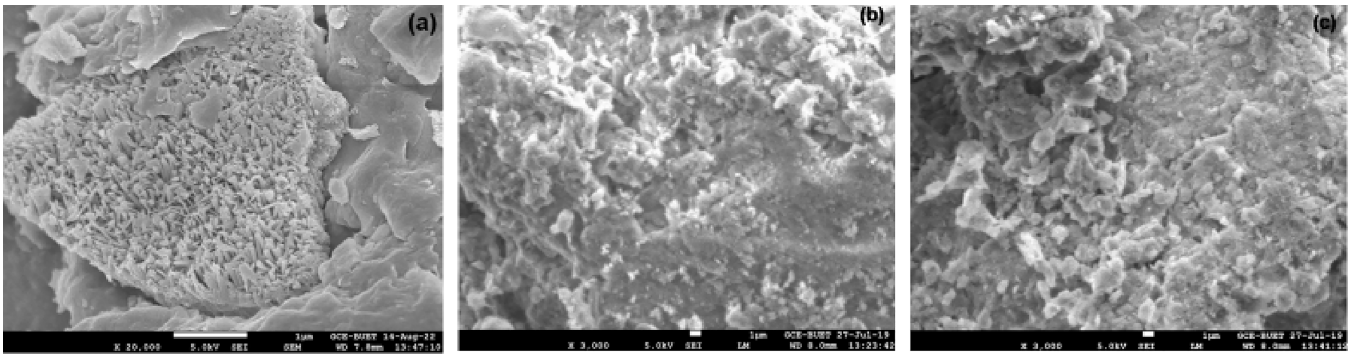

Figure 5. SEM images of (a) raw bentonite clay, (b) 3 M HNO_3-treated bentonite, and (c) 5 M HNO_3-treated bentonite.

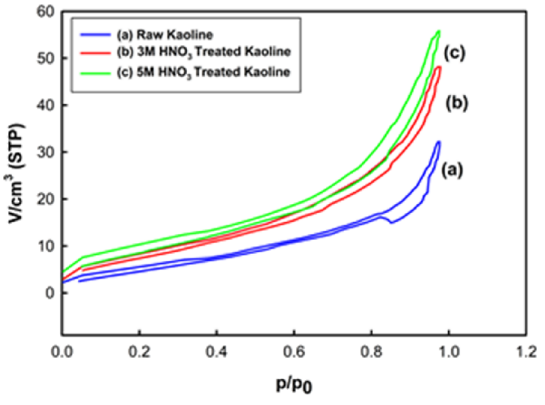

Figure 6. N_2 adsorption/desorption isotherms of (a) raw kaolin and (b) 3 and (c) 5 M nitric acid-treated kaolin.

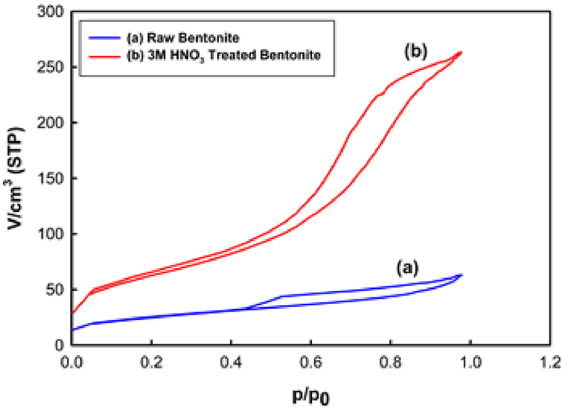

Figure 7. N_2 adsorption−desorption isotherms of (a) raw bentonite and (b) 3 M nitric acid-treated bentonite.

kaolin and bentonite are presented in Figures S1 and S2, respectively.

Figures 4 and 5 show the SEM images of raw and nitric acid-treated kaolin and bentonite, respectively. As can be seen from the SEM image of raw kaolin in Figure 4, the kaolin is crystalline with layered particles. Nevertheless, after acid treatment, the layered structures disappeared, likely attributed to the breakdown of the crystalline structure.

The SEM images of bentonite (Figure 5) indicate that acid treatment increased the roughness of the surface. The roughness is the consequence of surface etching, which intensified as the concentration of acid increased. Figures S3 and S4 represent the SEM images of the metal (Ni and Fe)- and bimetal (Ni−Fe)-impregnated kaolin and bentonite, respectively, at the magnification of ×20,000 at the scale of 1 μm. Bentonite surfaces are more rough compared to kaolin under similar conditions.

The BET analysis reveals that both kaolin and bentonite experience an augmentation in the specific surface area and pore diameter following the breakdown of their crystal structure and the leaching of Al_2O_3 caused by acid treatment (Table S1). The specific surface area of raw kaolin increases from 19.28 to 29.32 m^2/g (approximately 52% increase) and 33.08 m^2/g (approximately 72% increase) after treatment with 3 and 5 M nitric acid, respectively. In the case of raw bentonite, the specific surface area increases from 88.05 to 225.65 m^2/g (approximately 156% increase) after treatment (with 3 M nitric acid). The isotherms of both kaolin and bentonite exhibit type IV characteristics of mesoporous materials (Figures 6 and 7, respectively). Figure S5 shows the BJH pore size distribution of raw kaolin and 3 M HNO_3-treated and 5 M HNO_3-treated

https://doi.org/10.1021/acsomega.3c05951
ACS Omega 2024, 9, 474−485

Table 3. Liquid Obtained from Tire Pyrolysis Using Raw, Acid-Treated, and Metal-Impregnated Kaolin Catalysts at 500 °C (the Density of Liquid Is 0.94 g/mL)

	amount (g)			produced oil			
kaolin catalysts	catalyst[b]	waste tire	catalyst to tire ratio	mL	g	carbon black (g)	yield (%)
thermal (without catalyst)		30		13.50	12.69	12	42.30
raw kaolin	5	50	1:10	21	19.74	21	39.48
3 M HNO_3-treated kaolin	5	50	1:10	23	21.62	21	43.24
5 M HNO_3-treated kaolin	5	50	1:10	25	23.50	21	47
3 M HNO_3 kaolin + $Ca(OH)_2$	5 + 5	50	1:10	16	15.04	21	30
Ni/kaolin[a]	3	30	1:10	14.50	13.63	12.57	45.43
Fe/kaolin[a]	3	30	1:10	15	14.10	12.62	47
Ni/Fe/kaolin[a]	3	30	1:10	15	14.10	12.72	47

[a]Mono- and bimetals impregnated on 3 M nitric acid-treated kaolin. [b]The gaseous molecules were vented off. Each catalyst was used only once due to the deposition of coke on the surface.

Table 4. Liquid Obtained from Tire Pyrolysis Using Raw, Acid-Treated, and Metal-Impregnated Bentonite Catalysts at 500 °C (the Density of Liquid Is 0.93 g/mL)

	amount (g)			produced oil			
bentonite catalysts	catalyst[b]	waste tire	catalyst to tire ratio	mL	g	carbon black (g)	yield (%)
raw bentonite	5	50	1:10	17	15.81	21	31.62
3 M HNO_3-treated bentonite	5	50	1:10	19	17.67	21	35.34
5 M HNO_3-treated bentonite	5	50	1:10	21	19.53	21	39.06
3 M HNO_3-treated bentonite + $Ca(OH)_2$	5 + 5	50	1:10	16	14.88	21	29.76
Ni/bentonite[a]	3	30	1:10	13	12.09	12.39	40.30
Fe/bentonite[a]	3	30	1:10	13.50	12.55	12.42	41.85
Ni/Fe/bentonite[a]	3	30	1:10	11.50	10.69	12.02	35.65

[a]Mono- and bimetals impregnated on 3 M nitric acid-treated bentonite. [b]The gaseous molecules were vented off. Each catalyst was used only once due to the deposition of coke on the surface.

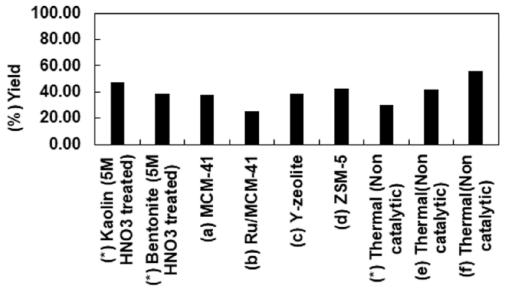

Figure 8. Comparison of oil yield with different catalysts. *This study. (a) Ref 15. (b) Ref 15. (c) Ref 14. (d) Ref 14. (e) Ref 15. (f) Ref 15.

Table 5. Sulfur Content in Oil % (w/w)

	sulfur content % (w/w) (method: IP61/59)					
	raw kaolin	3 M HNO_3-treated kaolin	3 M HNO_3-treated kaolin with $Ca(OH)_2$	raw bentonite	3 M HNO_3-treated bentonite	3 M HNO_3-treated bentonite with $Ca(OH)_2$
S%	1.12	1.10	0.95	1.15	1.13	0.60

kaolin. The average pore diameter of kaolin increases from 90.93 to 101.18 and 103.95 Å after treatment with 3 and 5 M HNO_3, respectively. Figure S6 shows the BJH pore size distribution of raw bentonite and 3 M HNO_3-treated bentonite, with the average pore diameter increasing from 44.18 to 71.86 Å after 3 M HNO_3 treatment.

As evidenced in Tables 3 and 4 , the percent yield of liquid increased compared to raw kaolin and raw bentonite due to the increment of specific surface area and pore diameter after acid treatment.

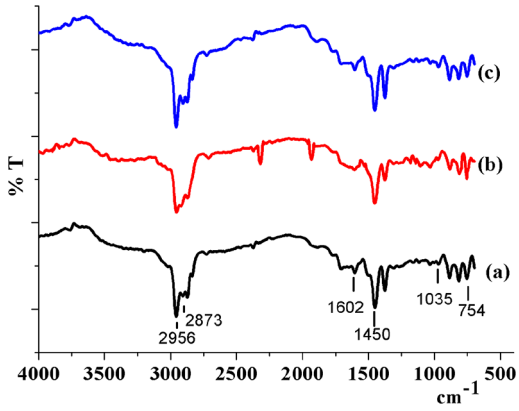

Figure 9. FTIR of tire-derived oil by kaolin catalysts: (a) raw kaolin, (b) 3 M HNO_3-treated kaolin, and (c) 3 M HNO_3-treated kaolin with $Ca(OH)_2$.

Waste Tire Pyrolysis Using Kaolin and Bentonite Catalysts. As a benchmark experiment, thermal pyrolysis of a 30 g waste tire was carried out at 500 °C under a N_2 atmosphere in the absence of a catalyst. This process resulted in 13.50 mL (12.69 g, density is 0.94 g/mL) of liquid representing a yield of 42.30%. Later, the waste tire was pyrolyzed, using raw kaolin (Si/Al ratio of 3.58) and raw bentonite (Si/Al ratio of 6.94) (Tables 3 and 4, respectively). The pyrolysis with raw kaolin produced a liquid yield of 39.48%, while raw bentonite resulted in a liquid yield of 31.62%. To investigate the influence of the Si/Al ratio on tire pyrolysis, raw kaolin and raw bentonite were treated with 3 and 5 M nitric acid. The treatment with HNO_3 of different concentrations caused an altered Si/Al ratio in kaolin and

https://doi.org/10.1021/acsomega.3c05951
ACS Omega 2024, 9, 474−485

Table 6. GC-MS Analysis of Liquid Obtained by Pyrolysis of Tire by Using Raw and Acid-Treated Kaolin Catalysts

name of compounds	% area		
	raw kaolin	3 M HNO_3-treated kaolin	3 M HNO_3-treated kaolin with $Ca(OH)_2$
limonene	12.34	20.27	39.76
1,2,3-trimethylindene		0.98	
1,3,6-heptatriene, 2,5,6-trimethyl-	1.04		
1*H*-indene, 1,1,3-trimethyl-	1.04		
1*H*-indene, 1,3-dimethyl-	0.7		
1*H*-indene, 1-ethyl-2,3-dihydro-1-methyl-	1.18		
1*H*-indene, 2,3-dihydro-1,1,5,6-tetramethyl-	0.67		
1*H*-indene, 2,3-dihydro-1,2-dimethyl-	1.39		
1*H*-indene, 2,3-dihydro-1,6-dimethyl-	1.93		
1*H*-indene, 2,3-dihydro-4,5,7-trimethyl-		1.07	
1*H*-indene, 2,3-dihydro-4-methyl-		0.71	
1*H*-indene, 2,3-dihydro-5-methyl-	1.52		
1*H*-indene, 3-ethenyl-2,3-dihydro-1,1-dimethyl-	0.73		
1*H*-indene,2,3-dihydro-2,2-dimethyl-		2.04	
2,6-dimethyl-1,3,5,7-octatetraene, *E,E*-		1.44	
benzene, (1-methyl-1-butenyl)-		1.36	
benzene, (2-methyl-1-propenyl)-	1.31		
benzene, (3-methyl-2-butenyl)-	0.7		
benzene, 1-(1,5-dimethyl-4-hexenyl)-4-methyl-	0.93	0.97	1.93
benzene, 1-(1,5-dimethylhexyl)-4-methyl-	1.14		
benzene, 1-(2-butenyl)-2,3-dimethyl-	1.02	0.71	
benzene, 1,2,3,5-tetramethyl-	2.45		
benzene, 1,2,4-trimethyl-	0.88		
benzene, 1,4-diethyl-	5.51		
benzene, 1-ethyl-3-methyl-	1.74	1.56	
benzene, 1-methyl-4-(1-methylethyl)-		0.93	
benzene, 1-methyl-4-(1-methylpropyl)-	0.64	1.20	
benzene, 2-ethenyl-1,4-dimethyl-		1.73	
benzene, 4-ethyl-1,2-dimethyl-		5.80	
benzothiazole	1.82		
cyclohexene, 1-methyl-4-(1-methylethylidene)-		1.54	
cyclopentane, 1-butyl-2-propyl-		1.61	
decane		1.04	
dodecane		0.63	
eicosane		0.68	1.31
heptadecane	1.34	2.25	
indane	0.64		
naphthalene, 1,2,3,4-tetrahydro-1,5-dimethyl-	0.83		
naphthalene, 1,2,3,4-tetrahydro-6,7-dimethyl-	0.66		
naphthalene, 1,2,3,4-tetramethyl-	1.97		
naphthalene, 1,2-dihydro-2,5,8-trimethyl-		0.66	
naphthalene, 1,2-dihydro-3-methyl-	0.59	1.38	
naphthalene, 1,3-dimethyl-	1.1		
naphthalene, 1,6,7-trimethyl-		3.05	1.97
naphthalene, 1,7-dimethyl-	1.06		
naphthalene, 1-methyl-	0.72		
naphthalene, 2,3,6-trimethyl-	2.17		
naphthalene, 2,6-dimethyl-	2.18	1.46	1.78
octane, 4-methyl-		2.67	
o-xylene	1.44		
pentadecane	1.94	1.47	
quinoline, 2,4-dimethyl-	4.91	4.96	6.44
tetradecane	0.97	1.51	

bentonite. The yield of liquid obtained by 3 and 5 M HNO_3-treated kaolin and bentonite catalysts is higher than that obtained with untreated kaolin and bentonite. For example, 3 M HNO_3-treated kaolin provided a 43.24% liquid yield, which increased to 47%, when using 5 M HNO_3 kaolin as opposed to the 39.48% liquid yield obtained with raw kaolin. Similarly, 3 M HNO_3-treated bentonite provided 35.34% liquid yield, which increased to 39%, when using 5 M HNO_3 bentonite as opposed to the 31.62% liquid yield obtained with raw bentonite.

To understand the effect of transition metals on tire pyrolysis, we impregnated monometals (Ni and Fe) and bimetals (Ni/Fe) on 3 M HNO_3-treated kaolin (Table 3) and bentonite (Table 4). The liquid yield increased with the impregnation of Ni and Fe on 3 M HNO_3-treated kaolin compared to pyrolysis by 3 M HNO_3-treated kaolin.

The Fe/kaolin catalyst performed better (47% liquid) than did the Ni/kaolin catalyst (45.43% liquid). Moreover, Ni/Fe/kaolin also produced 47% liquid. The metal-impregnated bentonite catalysts also increased the liquid yield, but the metal-impregnated kaolin catalysts performed better than the metal-impregnated bentonite catalysts. The liquid yield by Ni/bentonite and Fe/bentonite catalysts are 40.30 and 41.85%, respectively (Table 4), higher than the 35.34% obtained by 3 M HNO_3-treated bentonite.

In this study, kaolin catalysts provided a relatively higher amount of liquid compared to bentonite catalysts. The thermal process (without adding any catalysts) provided a 42.30% liquid. Other studies such as Dũng et al.[15] and Williams and Bridle[14] found a higher yield of liquid in the thermal process than in the catalytic process using MCM-41[15] and ZSM-5[14] catalysts, respectively (Figure 8). In thermal pyrolysis, Dũng et al.[15] obtained 42% liquid which decreased to 38 and 25% when using MCM-41[15] and Ru/MCM-41[15] catalysts, respectively (Figure 8). Similarly, Williams et al.[14] obtained 55.8% liquid in thermal pyrolysis, which decreased to 38.7 and 42.9% when Y-zeolite[14] and ZSM-5[14] catalysts were used, respectively (Figure 8). In the present study, the 5 M HNO_3-treated kaolin catalyst provided a higher yield of liquid (47%) compared to MCM-41,[15] Ru/MCM-41,[15] Y-zeolite,[14] and ZSM-5[14] catalysts, which provided 38, 25, 38.7, and 42.9%, respectively. Additionally, in this study, the Fe/kaolin and Ni/Fe/kaolin catalysts also provided 47% liquid, higher than those of MCM-41 and ZSM-5.

Typical sulfur content in raw tires is about 1.6%. Sulfur could be removed by employing calcium hydroxide. In our experiments, we conducted tire pyrolysis, using a mixture of

https://doi.org/10.1021/acsomega.3c05951
ACS Omega 2024, 9, 474−485

Table 7. GC-MS Analysis of Liquid Obtained by Pyrolysis of Tire by Using Raw and Acid-Treated Bentonite Catalysts

Name of Compounds	% area		
	raw bentonite	3 M HNO_3-treated bentonite	3 M HNO_3-treated bentonite with Ca $(OH)_2$
limonene	9.33	37.69	33.46
1*H*-indene, 1,3-dimethyl-	0.57		
1*H*-indene, 1-ethyl-2,3-dihydro-1-methyl-	0.68		
1*H*-indene, 2,3-dihydro-1,1,5,6-tetramethyl-	0.65		
1*H*-indene, 2,3-dihydro-1,2-dimethyl-		1.52	1.59
1*H*-indene, 2,3-dihydro-1,3-dimethyl-	1.22		
1*H*-indene, 2,3-dihydro-1,6-dimethyl-	1.51		
1*H*-indene, 2,3-dihydro-5-methyl-	1.17		
1*H*-indene, 3-ethenyl-2,3-dihydro-1,1-dimethyl-	0.73		
1-pentadecene	1.12		
2-ethyl-2,3-dihydro-1*H*-indene	0.54		
2-methylindene			1.10
3-(2-methyl-propenyl)-1*H*-indene			
benzene, (2-methyl-1-propenyl)-	0.78		
benzene, 1-(1,5-dimethylhexyl)-4-methyl-	1.5		
benzene, 1,2,4,5-tetramethyl-	0.54		
benzene, 1,3,5-trimethyl-2-(1,2-propadienyl)-			1.05
benzene, 1-ethyl-3-methyl-	0.99		
benzene, 1-methyl-3-(1-methylethyl)-		3.26	2.47
benzene, 1-methyl-4-(1-methylpropyl)-	0.53		
benzene, 1-methyl-4-[(methylthio)ethynyl]-			1.61
benzene, 2,4-diethyl-1-methyl-	0.81		
benzo[*b*]thiophene, 2-ethyl-5,7-dimethyl-			
benzocycloheptatriene			1.60
benzothiazole	1.13	1.79	1.41
benzothiazole, 2-methyl-		1.47	
dodecane	0.48		
heptadecane			1.08
hexacosane			1.19
hexadecane			
naphthalene, 1,2,3,4-tetrahydro-5-methyl-	1.13		1.86
naphthalene, 1,2,3,4-tetramethyl-			
naphthalene, 1,2-dihydro-3-methyl-			1.01
naphthalene, 1,4,6-trimethyl-			
naphthalene, 1,6,7-trimethyl-		1.95	1.95
naphthalene, 1-methyl-	0.72		
naphthalene, 2,3,6-trimethyl-			
naphthalene, 2,3-dimethyl-	0.98		
naphthalene, 2,6-dimethyl-	2.13		
naphthalene, 2,7-dimethyl-		1.86	1.89
octadecane	0.73		
o-cymene	5.44		
o-xylene	0.75		
pentadecane	2.21		
pentadecane		1.35	1.21
quinoline, 2,4-dimethyl-	5.1	6.25	6.15

kaolin and $Ca(OH)_2$ as well as bentonite and $Ca(OH)_2$. Table 5 shows the kaolin and bentonite catalysts as well as use of $Ca(OH)_2$ mixed with kaolin and bentonite, which reduced sulfur content significantly. The S% by the raw kaolin catalyst is 1.12%. When 3 M HNO_3 acid-treated kaolin mixed with $Ca(OH)_2$, the S% reduced to 0.95%. Similarly, the S% by raw bentonite was 1.15%. When 3 M HNO_3 acid-treated bentonite mixed with the $Ca(OH)_2$, the S% reduced to 0.60%.

The FTIR analysis reveals the presence of alkanes and alkenes in the liquid as demonstrated in Figure 9 and Figure S7, respectively. The existence of C−H stretching of methyl and methylene groups of alkane is indicated by the % transmittance peak values at the wavenumbers of 2956 and 2873 cm^{-1}. Additionally, the wavenumber at 1602 cm^{-1} was due to C═C stretching and the 1450 cm^{-1} band is attributed to C−H scissoring. Furthermore, C−H bending was observed at 1035 and 754 cm^{-1}. The liquid does not contain any aldehyde or ketone group. The compositions of the oil remain unchanged even with the addition of $Ca(OH)_2$. The impregnation of monometals (Ni and Fe) and bimetals (Ni/Fe) on acidified kaolin (Figure S8) and bentonite (Figure S9) also indicates the presence of alkanes and alkenes in the liquid.

Figures S10 and S11 display the ^1H NMR spectra of the liquid obtained from tire pyrolysis using kaolin and bentonite catalysts, respectively. The multiplets around 7.5 ppm indicate the presence of aromatic protons. Note that the multiplets at 1−2.5 ppm originate from various alkane substituents. The peaks at 4.2 and 4.7 ppm originate from double-bonded CH protons in the cyclohexene ring and the terminal double bond of limonene. The GC-MS analysis of the liquid obtained from tire pyrolysis using raw kaolin and acid-treated kaolin (Table 6) as well as raw bentonite and acid-treated bentonite (Table 7) reveals that the liquid primarily consists of limonene, alkylated benzene, alkylated indene, alkylated naphthalene, and a small amount of alkanes.

The Ni/kaolin and Ni/bentonite catalysts yielded a higher proportion of branched compounds compared to the acid-treated kaolin and bentonite catalysts, as indicated in Table S3. Specifically, the Ni/kaolin and Ni/bentonite catalysts produced more branched benzene, alkyl-substituted naphthalene, substituted indene, and alkyl-substituted cyclohexene. However, no limonene was observed in the products obtained from the Ni/kaolin and Ni/bentonite catalysts.

The produced oil contains a higher content of aromatic compounds. Pakdel et al.[23] and Frigo et al.[24] reported that tire oil consisting of cyclic and aromatic hydrocarbons can be used as a component of motor fuels or as a feedstock for petrochemical processes. At present, the waste tire pyrolysis oil is being used as fuel in heavy industries such as cement plants, glass factories, ceramic factories, brick factories, heavy oil power plants, steel factories, and boiler factories. In addition, gas chromatography−mass spectrometry (GC-MS)

https://doi.org/10.1021/acsomega.3c05951
ACS Omega 2024, 9, 474−485

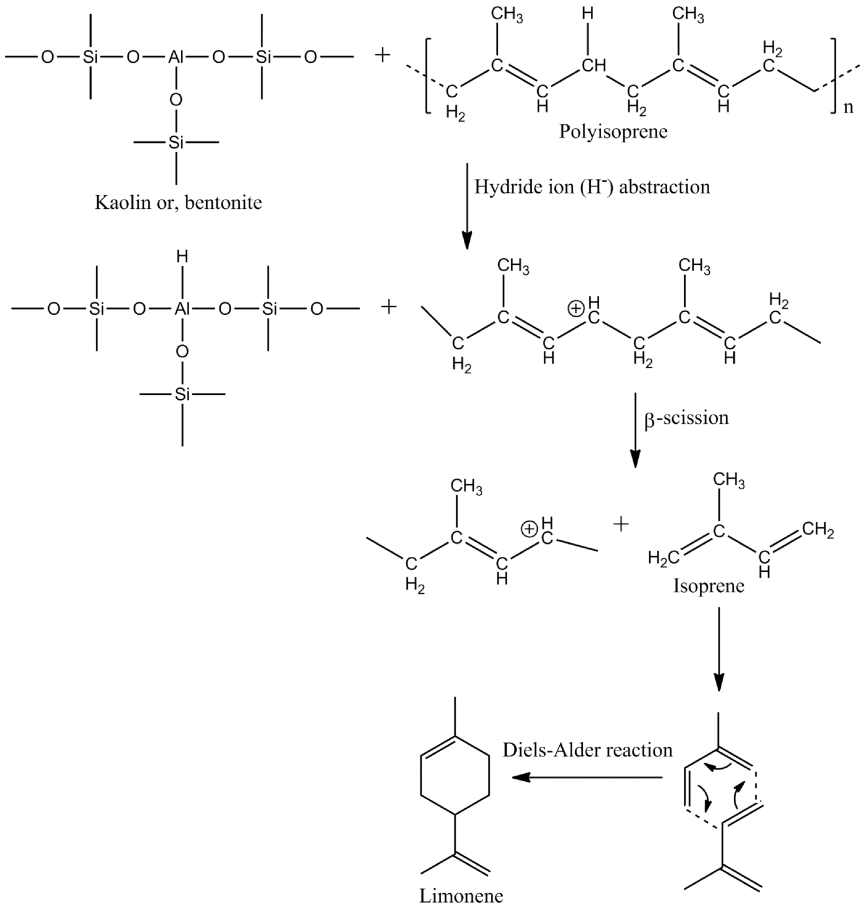

Figure 10. Proposed mechanism of formation of limonene through carbocation formed by a kaolin or bentonite catalyst. This mechanism is in good agreement with the mechanism of the ZSM-5 zeolite catalyst.[4]

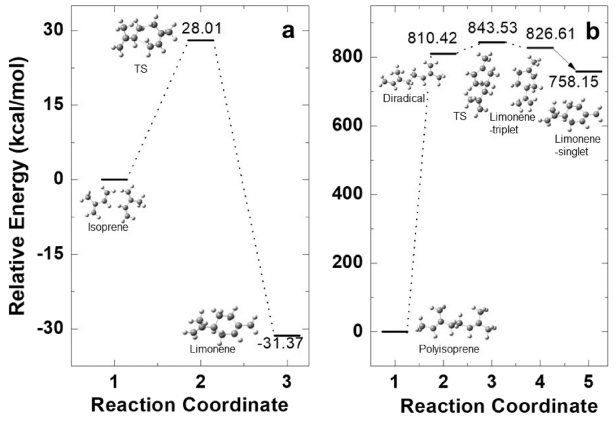

Figure 11. Relative energy profile of limonene: (a) energy of the reaction path of limonene from two isoprene molecules and (b) energy of dimeric species, having diradicals from polyisoprene.

analysis confirmed the presence of limonene, a crucial ingredient for commercial perfume production, in the liquid products.

Mechanism of Tire Pyrolysis. Kaolin and bentonite clay catalysts are acidic aluminosilicate. The presence of the Al^{3+} ion provides Lewis acid sites in the catalyst. Thus, we believe that in the presence of a clay catalyst, carbenium ion might form due to abstraction of hydride ion from polyisoprene by Lewis acid sites on clay and successive β scission might occur to form isoprene molecules[4] (Figure 10). Two isoprene molecules can undergo a Diels−Alder cyclization reaction to produce limonene. During cracking isomerization, hydrogen transfer, cyclization, and aromatization might also occur, leading to formation of various products.[4] Our proposed mechanism is in good agreement with the mechanism proposed by the ZSM-5 zeolite catalyst where a carbenium ion is believed to be formed during catalytic pyrolysis.[4,11,25] For thermal pyrolysis, two different mechanisms were proposed for the degradation of tire and the formation of limonene (Figures S12 and S13).[26]

As two different mechanisms are proposed for the formation of limonene, we investigated which path is more probable by using density functional theory (DFT). The limonene formation mechanism from two isoprene molecules and

Table 8. Fuel Parameters of Tire Oil Obtained by Kaolin and Bentonite Catalysts

test parameter	method	oil by kaolin catalyst	oil by bentonite catalyst
density, g/cm^3	ASTM D1298	0.94	0.93
kinematic viscosity, mm^2/s (at 40 °C)	ASTM D445	3.13	3.05
calorific value, kcal/kg	BOMB calorimeter	13,922	10,174
flashpoint, °C	ASTMD 93−62	60	59
pour point, °C	ASTMD 97−57	<−6	<−5

https://doi.org/10.1021/acsomega.3c05951
ACS Omega 2024, 9, 474−485

dimer species with diradical has been studied using the B3LYP/6-31+G(d,p) level of theory. Intrinsic reaction coordinates (IRC) and the Gonzalez-Schlegel[27] second-order method was used to follow the minimum energy paths. All the necessary calculations were completed using the Gaussian 16 program.[28]

When limonene is produced from two isoprene molecules through the Diels−Alder cyclization reaction, the intermediates undergo a transition state of 28.01 kcal/mol liberating 31.37 kcal/mol (exothermic reaction) (Figure 11a). This pathway is both kinetically and thermodynamically accessible. On the other hand, when limonene is produced from dimeric species having diradicals (810.42 kcal/mol), the intermediate undergoes a transition state (839.33 kcal/mol) that converts limonene into a triplet ground state (826.61 kcal/mol) (Figure 11b). Finally, the triplet ground state reaches the singlet ground state (endothermic reaction) by liberating 68.61 kcal/mol energy. This pathway is unlikely to produce limonene because of the requirement of large activation energy.

In this study, we used kaolin and bentonite clay catalysts for tire pyrolysis. The kaolin and bentonite clay catalysts are acidic aluminosilicate, which is attributed to the presence of Al^{3+} ion leading to the provision of Lewis acid sites in the catalysts. Our hypothesis is that clay catalysts may facilitate the formation of a carbocation, which, in turn, promotes the generation of isoprene molecules. Consequently, two isoprene molecules can then undergo a Diels−Alder cyclization reaction, resulting in the production of limonene.

Table 8 presents the fuel parameter values obtained from the experiments. The density of liquid obtained by kaolin and bentonite are found to be 0.94 and 0.93 g/cm^3, respectively. The calorific value of the liquid obtained by kaolin is found to be higher than that of the liquid obtained by bentonite catalyst. The calorific value was measured with a bomb calorimeter. The calorific values were found to be 13,922 and 10,174 kcal/kg, and flash points were 60 and 59 °C for the liquid obtained by kaolin and bentonite catalysts, respectively.

CONCLUSIONS

In this study, kaolin and bentonite clay-based catalysts have been investigated in the pyrolysis of waste tire to produce higher amounts of liquid hydrocarbons. Acid-treated kaolin yielded higher liquid hydrocarbons (43.24−47%) compared to acid-treated bentonite (35.34−41.85%). Among the metal-impregnated catalysts, Fe/kaolin and Ni/Fe/kaolin demonstrated higher liquid yields (47%) than the conventional catalysts MCM-41 (38%) and ZSM-5 (42.9%). The GC-MS analysis confirmed the formation of limonene through Diels−Alder cyclization reaction of two isoprene molecules when acid-treated kaolin and bentonite clay were used as catalysts. However, metal-impregnated clay catalysts (such as Ni/kaolin and Ni/bentonite) did not produce limonene. The addition of $Ca(OH)_2$ with kaolin and bentonite during pyrolysis reduced the sulfur content in the oil. The calorific values of oil obtained by kaolin and bentonite catalysts are 13,922 and 10,174 kcal/kg, respectively.

ASSOCIATED CONTENT

Supporting Information

The Supporting Information is available free of charge at https://pubs.acs.org/doi/10.1021/acsomega.3c05951.

XRD of metal-impregnated kaolin: Ni/kaolin, Fe/kaolin, and Ni/Fe/kaolin; XRD of metal-impregnated bentonite: Ni/bentonite, Fe/bentonite, and Ni/Fe/bentonite; SEM images of metal-impregnated kaolin: Ni/kaolin, Fe/kaolin, and Ni/Fe/kaolin, magnification ×20,000, scale 1 μm; SEM images of metal-impregnated bentonite: Ni/bentonite, Fe/bentonite, and Ni/Fe/bentontie, magnification ×20,000, scale 1 μm; BJH pore size distribution of raw kaolin, 3 M, and 5 M nitric acid-treated kaolin; BJH pore size distribution of raw bentonite and 3 M nitric acid-treated bentonite; FTIR of tire-derived oil by bentonite catalysts: raw bentonite, 3 M HNO_3-treated bentonite, and 3 M HNO_3-treated bentonite with $Ca(OH)_2$; FTIR of tire-derived oil by metal-impregnated kaolin catalysts: Ni/kaolin, Fe/kaolin, and Ni/Fe/kaolin; FTIR of tire-derived oil by metal-impregnated bentonite catalysts: Ni/bentonite, Fe/bentonite, and Ni/Fe/bentonite; ^{1}HNMR of liquid obtained by pyrolysis of tire by raw kaolin, 3 M HNO_3-treated kaolin, and 3 M HNO_3-treated kaolin with $Ca(OH)_2$; ^{1}H NMR of liquid obtained by pyrolysis of tire by raw bentonite, 3 M HNO_3-treated bentonite, and 3 M HNO_3-treated bentonite with $Ca(OH)_2$; postulated mechanism of degradation of natural rubber and formation of limonene;[23] postulated mechanism of formation of the dimer with diradicals and cyclization forming limonene;[23] summary of BET results of raw bentonite, raw kaolin, and acid-treated bentonite and kaolin; and GC-MS analysis of liquid obtained by pyrolysis of tire by using Ni/kaolin and Ni/bentonite catalysts (PDF)

AUTHOR INFORMATION

Corresponding Author

Mahmudur Rahman − *Department of Chemistry, Jagannath University, Dhaka 1100, Bangladesh; Department of Chemistry, Bangladesh University of Engineering and Technology (BUET), Dhaka 1000, Bangladesh; HPE Project Services, Ashfield NSW 2131, Australia; Institute of Fuel Research and Development (IFRD), Bangladesh Council of Scientific and Industrial Research (BCSIR), Dhaka 1205, Bangladesh; Bangladesh Reference Institute for Chemical Measurements, Bangladesh Council of Scientific and Industrial Research (BCSIR), Dhaka 1205, Bangladesh; Institute of Glass and Ceramic Research and Testing (IGCRT), Bangladesh Council of Scientific and Industrial Research (BCSIR), Dhaka 1205, Bangladesh; Department of Biochemistry and Microbiology, North South University, Dhaka 1100, Bangladesh;* orcid.org/0000-0001-6008-4558; Email: mahmudur.rahman@chem.jnu.ac.bd, mm_rahman1978@yahoo.co.uk

Authors

Muhammad Omar Faruk − *Department of Chemistry, Bangladesh University of Engineering and Technology (BUET), Dhaka 1000, Bangladesh*

Md Waliul Islam − *HPE Project Services, Ashfield NSW 2131, Australia*

Moni Akter − *Department of Chemistry, Jagannath University, Dhaka 1100, Bangladesh*

Joyanta K. Saha − *Department of Chemistry, Jagannath University, Dhaka 1100, Bangladesh;* orcid.org/0000-0002-5592-2577

https://doi.org/10.1021/acsomega.3c05951
ACS Omega 2024, 9, 474−485

Nafees Ahmed − *Department of Chemistry, Jagannath University, Dhaka 1100, Bangladesh*
Ayesha Sharmin − *Department of Chemistry, Bangladesh University of Engineering and Technology (BUET), Dhaka 1000, Bangladesh*
Md. Azizul Hoque − *Institute of Fuel Research and Development (IFRD), Bangladesh Council of Scientific and Industrial Research (BCSIR), Dhaka 1205, Bangladesh*
Mirola Afroze − *Bangladesh Reference Institute for Chemical Measurements, Bangladesh Council of Scientific and Industrial Research (BCSIR), Dhaka 1205, Bangladesh*
Mala Khan − *Bangladesh Reference Institute for Chemical Measurements, Bangladesh Council of Scientific and Industrial Research (BCSIR), Dhaka 1205, Bangladesh*
Umme Sarmeen Akhtar − *Institute of Glass and Ceramic Research and Testing (IGCRT), Bangladesh Council of Scientific and Industrial Research (BCSIR), Dhaka 1205, Bangladesh*
Md Mainul Hossain − *Department of Biochemistry and Microbiology, North South University, Dhaka 1100, Bangladesh*

Complete contact information is available at: https://pubs.acs.org/10.1021/acsomega.3c05951

Notes

The authors declare no competing financial interest.

■ ACKNOWLEDGMENTS

The authors sincerely acknowledge the financial support provided by Jagannath University, Dhaka, Bangladesh. They also extend their gratitude to Mihir Kanti Choudhury from Metropolitan University, Sylhet, Bangladesh, for proofreading assistance.

■ REFERENCES

(1) Tian, X.; Han, S.; Wang, K.; Shan, T.; Li, Z.; Li, S.; Wang, C. Waste resource utilization: Spent FCC catalyst-based composite catalyst for waste tire pyrolysis. *Fuel* **2022**, *328*, No. 125236.
(2) Zhang, X.; Tang, J.; Chen, J. Behavior of sulfur during pyrolysis of waste tires: A critical review. *Journal of the Energy Institute* **2022**, *102*, 302−314.
(3) Islam, M. R.; Islam, M. N.; Mustafi, N. N.; Rahim, M. A.; Haniu, H. Thermal Recycling of Solid Tire Wastes for Alternative Liquid Fuel: The First Commercial Step in Bangladesh. *Procedia Engineering* **2013**, *56*, 573−582.
(4) Arabiourrutia, M.; Lopez, G.; Artetxe, M.; Alvarez, J.; Bilbao, J.; Olazar, M. Waste tyre valorization by catalytic pyrolysis − A review. *Renewable and Sustainable Energy Reviews* **2020**, *129*, No. 109932.
(5) Martínez, J. D.; Puy, N.; Murillo, R.; García, T.; Navarro, M. V.; Mastral, A. M. Waste tyre pyrolysis − A review. *Renewable and Sustainable Energy Reviews* **2013**, *23*, 179−213.
(6) Yu, J.; Liu, S.; Cardoso, A.; Han, Y.; Bikane, K.; Sun, L. Catalytic pyrolysis of rubbers and vulcanized rubbers using modified zeolites and mesoporous catalysts with Zn and Cu. *Energy* **2019**, *188*, No. 116117.
(7) Chao, L.; Zhang, C.; Zhang, L.; Gholizadeh, M.; Hu, X. Catalytic pyrolysis of tire waste: Impacts of biochar catalyst on product evolution. *Waste Management* **2020**, *116*, 9−21.
(8) Duanguppama, K.; Pannucharoenwong, N.; Echaroj, S.; Pham, L. K. H.; Samart, C.; Rattanadecho, P. Integrated catalytic pyrolysis and catalytic upgrading of Leucaena leucocephala over natural catalysts. *Journal of the Energy Institute* **2023**, *106*, No. 101155.
(9) Sanchís, A.; Veses, A.; Martínez, J. D.; López, J. M.; García, T.; Murillo, R. The role of temperature profile during the pyrolysis of end-of-life-tyres in an industrially relevant conditions auger plant. *Journal of Environmental Management* **2022**, *317*, No. 115323.
(10) Lopez, G.; Alvarez, J.; Amutio, M.; Mkhize, N. M.; Danon, B.; van der Gryp, P.; Görgens, J. F.; Bilbao, J.; Olazar, M. Waste truck-tyre processing by flash pyrolysis in a conical spouted bed reactor. *Energy Conversion and Management* **2017**, *142*, 523−532.
(11) Kaminsky, W. Thermal recycling of polymers. *Journal of Analytical and Applied Pyrolysis* **1985**, *8*, 439−448.
(12) Banar, M.; Akyıldız, V.; Özkan, A.; Çokaygil, Z.; Onay, Ö. Characterization of pyrolytic oil obtained from pyrolysis of TDF (Tire Derived Fuel). *Energy Conversion and Management* **2012**, *62*, 22−30.
(13) Unapumnuk, K.; Lu, M.; Keener, T. C. Carbon Distribution from the Pyrolysis of Tire-Derived Fuels. *Ind. Eng. Chem. Res.* **2006**, *45* (26), 8757−8764.
(14) Williams, P. T.; Brindle, A. J. Catalytic pyrolysis of tyres: influence of catalyst temperature. *Fuel* **2002**, *81* (18), 2425−2434.
(15) Dũng, N. A.; Klaewkla, R.; Wongkasemjit, S.; Jitkarnka, S. Light olefins and light oil production from catalytic pyrolysis of waste tire. *Journal of Analytical and Applied Pyrolysis* **2009**, *86* (2), 281−286.
(16) Zhang, X.; Wang, T.; Ma, L.; Chang, J. Vacuum pyrolysis of waste tires with basic additives. *Waste Management* **2008**, *28* (11), 2301−2310.
(17) Hakeem, I. G.; Aberuagba, F.; Musa, U. Catalytic pyrolysis of waste polypropylene using Ahoko kaolin from Nigeria. *Applied Petrochemical Research* **2018**, *8* (4), 203−210.
(18) Rahman, M.; SHUVA, Z. M.; Rahman, M. A.; Ahmed, N.; Sharmin, A.; Laboni, A. A.; Khan, M.; Islam, M. W.; Al-Mamun, M.; Roy, S. C.; Saha, J. K. Catalytic pyrolysis of single-use waste polyethylene for the production of liquid hydrocarbon using modified bentonite catalyst. *Eur. J. Inorg. Chem.* **2022**, No. e202200409, DOI: 10.1002/ejic.202200409.
(19) Luo, W.; Wan, J.; Fan, Z.; Hu, Q.; Zhou, N.; Xia, M.; Song, M.; Qi, Z.; Zhou, Z. In-situ catalytic pyrolysis of waste tires over clays for high quality pyrolysis products. *Int. J. Hydrogen Energy* **2021**, *46* (9), 6937−6944.
(20) Ahmad, I.; Khan, M. I.; Khan, H.; Ishaq, M.; Tariq, R.; Gul, K.; Ahmad, W. Influence of metal-oxide-supported bentonites on the pyrolysis behavior of polypropylene and high-density polyethylene. *J. Appl. Polym. Sci.* 2015, *132*, 1, DOI: 10.1002/app.41221.
(21) Souza, K. R.; de Lima, A. F. F.; de Sousa, F. F.; Appel, L. G. Preparing Au/ZnO by precipitation−deposition technique. *Applied Catalysis A: General* **2008**, *340* (1), 133−139.
(22) (a) Al-asadi, M.; Miskolczi, N. High Temperature Pyrolysis of Municipal Plastic Waste Using Me/Ni/ZSM-5 Catalysts: The Effect of Metal/Nickel Ratio. *Energies* **2020**, *13* (5), 1284. (b) Al-asadi, M.; Miskolczi, N.; Eller, Z. Pyrolysis-gasification of wastes plastics for syngas production using metal modified zeolite catalysts under different ratio of nitrogen/oxygen. *Journal of Cleaner Production* **2020**, *271*, No. 122186.
(23) Pakdel, H.; Pantea, D. M.; Roy, C. Production of dl-limonene by vacuum pyrolysis of used tires. *Journal of Analytical and Applied Pyrolysis* **2001**, *57* (1), 91−107.
(24) Frigo, S.; Seggiani, M.; Puccini, M.; Vitolo, S. Liquid fuel production from waste tyre pyrolysis and its utilisation in a Diesel engine. *Fuel* **2014**, *116*, 399−408.
(25) Corma, A.; Orchillés, A. V. Current views on the mechanism of catalytic cracking. *Microporous Mesoporous Mater.* **2000**, *35*−*36*, 21−30.
(26) (a) Pakdel, H.; Roy, C.; Aubin, H.; Jean, G.; Coulombe, S. Formation of dl-limonene in used tire vacuum pyrolysis oils. *Environ. Sci. Technol.* **1991**, *25* (9), 1646−1649. (b) Mastral, A. M.; Murillo, R.; Callén, M. S.; García, T.; Snape, C. E. Influence of Process Variables on Oils from Tire Pyrolysis and Hydropyrolysis in a Swept Fixed Bed Reactor. *Energy Fuels* **2000**, *14* (4), 739−744.
(27) (a) Gonzalez, C.; Schlegel, H. B. Reaction path following in mass-weighted internal coordinates. *J. Phys. Chem.* **1990**, *94* (14), 5523−5527. (b) Gonzalez, C.; Schlegel, H. B. Improved algorithms for reaction path following: Higher-order implicit algorithms. *J. Chem. Phys.* **1991**, *95* (8), 5853−5860.

(28) Frisch, M. J.; Trucks, G. W.; Schlegel, H. B.; Scuseria, G. E.; Robb, M. A.; Cheeseman, J. R.; Scalmani, G.; Barone, V.; Petersson, G. A.; Nakatsuji, H.; Li, X.; Caricato, M.; Marenich, A. V.; Bloino, J.; Janesko, B. G.; Gomperts, R.; Mennucci, B.; Hratchian, H. P.; Ortiz, J. V.; Izmaylov, A. F.; Sonnenberg, J. L.; Williams; Ding, F.; Lipparini, F.; Egidi, F.; Goings, J.; Peng, B.; Petrone, A.; Henderson, T.; Ranasinghe, D.; Zakrzewski, V. G.; Gao, J.; Rega, N.; Zheng, G.; Liang, W.; Hada, M.; Ehara, M.; Toyota, K.; Fukuda, R.; Hasegawa, J.; Ishida, M.; Nakajima, T.; Honda, Y.; Kitao, O.; Nakai, H.; Vreven, T.; Throssell, K.; Montgomery, Jr., J. A.; Peralta, J. E.; Ogliaro, F.; Bearpark, M. J.; Heyd, J. J.; Brothers, E. N.; Kudin, K. N.; Staroverov, V. N.; Keith, T. A.; Kobayashi, R.; Normand, J.; Raghavachari, K.; Rendell, A. P.; Burant, J. C.; Iyengar, S. S.; Tomasi, J.; Cossi, M.; Millam, J. M.; Klene, M.; Adamo, C.; Cammi, R.; Ochterski, J. W.; Martin, R. L.; Morokuma, K.; Farkas, O.; Foresman, J. B.; Fox, D. J. *Gaussian 16*; Gaussian Inc.: Wallingford, CT, 2016.

https://doi.org/10.1021/acsomega.3c05951
ACS Omega 2024, 9, 474−485